Direct verification of the fluctuation-response relation in viscously coupled oscillators

Shuvojit Paul,[1] Abhrajit Laskar,[2] Rajesh Singh,[2] Basudev Roy,[3] R. Adhikari,[2,4,*] and Ayan Banerjee[1,†]

[1] *Indian Institute of Science Education and Research, Kolkata*
[2] *The Institute of Mathematical Sciences-HBNI, CIT Campus, Tarmani, Chennai 600113, India*
[3] *Department of Physics, Indian Institute of Technology Madras, Chennai 600036, India*
[4] *DAMTP, Centre for Mathematical Sciences, University of Cambridge, Wilberforce Road, Cambridge CB3 0WA, UK*

(Dated: June 30, 2017)

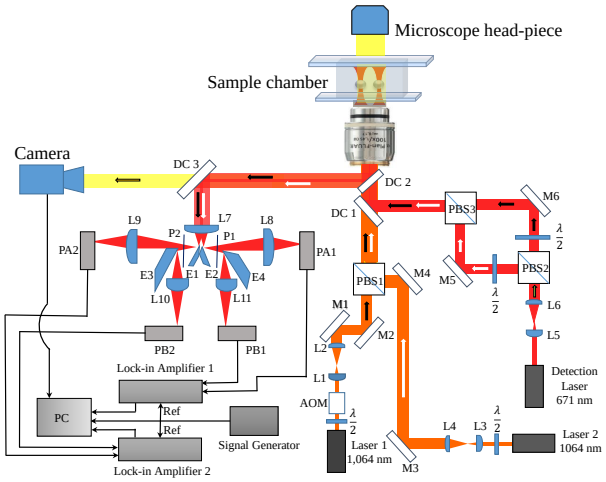

Figure 1. A detailed schematic of the setup is shown. Key: $\frac{\lambda}{2}$: half-wave plate, L: lens, M: mirror, AOM: accousto optical modulator, PBS: polarising beam splitter, DC: dicroic mirror respectively, E: edge mirror, P: polariser, PA, PB: photodiodes.

SUPPLEMENTARY INFORMATION

A. Experiment

We set up a dual-beam optical tweezers (Fig. 1) by focusing two orthogonally polarized beams of wavelength $\lambda = 1064$ nm generated independently from two diode lasers using a high NA immersion-oil microscope objective (Zeiss PlanApo,100 $\times$ 1.4). An AOM, located conjugate to the back-focal plane of the objective using the telescopic lens pair L1-L2 (see Fig. 1), is used for modulating one of the traps. A long optical path after the AOM ensures that a minimal beam deflection is enough to modulate one of the trapped beams, so that the intensity in the first order remains constant to around 2%. The modulated and unmodulated beams are independently steered using mirror pairs M1, M2 and M3, M4, respectively, and coupled into a polarizing beam splitter (PBS1). For detection, we use a separate laser of wavelength $\lambda = 671$ nm, that is again divided into two beams of orthogonal polarization by PBS2 and coupled into PBS3. We then use a dichroic (DC1) to overlap the two pairs of trapping and detection beams into the optical tweezers microscope (Zeiss Axiovert.A1). two trapped beads are imaged and their displacements measured by back-focal- plane-interferometry, while the white light for imaging and the detection laser beams are separated by dichroics DC2 and DC3, respectively. A very low volume fraction sample ($\phi \approx 0.01$) is prepared with 3 μm diameter polystyrene latex beads in 1 M NaCl-water solution for avoiding surface charges. A single droplet of about 20 μl volume of the sample is introduced in a sample chamber made out of a standard 10 mm square cover slip attached by double-sided sticky tape to a microscope slide. We trap two spherical polystyrene beads (Sigma LB-30) of mean size 3 μm each, in two calibrated optical traps which are separated by a distance 4 ± 0.1 μm, so that the surface-surface distance of the trapped beads is 1 ± 0.2 μm, and the distance from the cover slip surface is 30 μm. From the literature, this distance is still large enough to avoid optical cross talk and effects due to surface charges [1]. In order to ensure that the trapping beams do not influence each other, we measure the Brownian motion of one when the other is switched on (in the absence of a particle), and check that there are no changes in the Brownian motion. One of the traps is sinusoidally modulated and the phase and amplitude response of both the driving and driven particles with reference to the sinusoidal drive are measured by lock-in detection (Stanford Research, SR830). To get large signal to noise, we use balanced detection using photodiode pairs PA1, PB1 and PA2, PB2, for the driving and driven particles, respectively. The two beams for balanced detection are prepared by edge mirrors E1, E3 (E2, E4) for the driving (driven) particle, respectively. Polarizers P1 (P2) are aligned in such a way so as select the desired polarization component of the detection beams that are prepared, as mentioned above, in orthogonal polarization states for the driving (driven) particle. Thus, we use a combination of orthogonal polarization and dichroic beam splitters to separate out the detection beams for the driving and driven particles, respectively. The voltage-amplitude calibration of our detection system reveals that we can resolve motion of around 5 nm with an SNR of 2.

Fig. 2 (a) and (b) shows the histogram of position coordinate data that we acquire for the Brownian motion of driving particle B1 and driven particle B2, re-

* rjoy@imsc.res.in
† ayan@iiserkol.ac.in

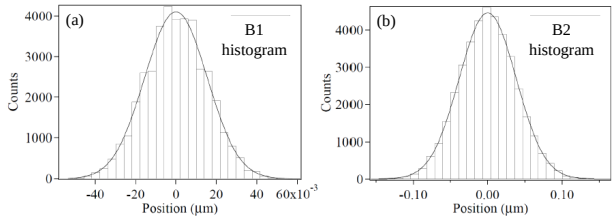

Figure 2. Position histograms of (a) B1 (driving particle) and (b) B2 (driven particle). The solid black lines are corresponding Gaussian fits which show that the potentials are harmonic in nature.

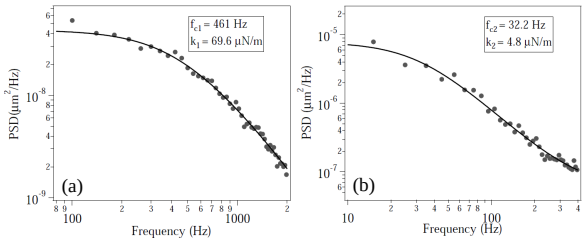

Figure 3. Calibration of traps for B1 and B2. Experimentally measured data points are shown in filled gray circles, whereas the Lorentzian fit is denoted by the solid black line. (a) PSD for B1 which has a corner frequency $f_{c1} = 461$Hz and stiffness $k_1 = 69.6\,\mu$N/m. (b) PSD for B2 which has a corner frequency $f_{c1} = 32.2$Hz and stiffness $k_1 = 4.8\,\mu$N/m.

spectively. As is clear, the data are normally distributed in both traps and fit very well to Gaussians (shown in bold lines). To calibrate the traps and determine the trap stiffnesses, we measure the power spectral density (PSD) of the Brownian motion of each particle in the absence of the other. The results are shown in Fig. A(a) and (b). Each PSD is obtained by data blocking 100 points in the manner described in Ref. \cite{flyvbjerg}. The Lorentzian fits to the data are good, and we obtain corner frequencies f_{c1} =461 Hz and f_{c2} =32.2 Hz for particles B1 and B2, which yield stiffnesses of k_1 =69.2 Hz and k_2= 4.8 Hz, respectively. For the two particle correlation experiments, as a consistency check, we determine the position cross-correlation function in time domain for B1 and B2 as shown in Fig. A. The data fits well to Eq.5 in Ref. [2], with the constant parameters appropriately calculated for our case. Finally, we demonstrate the amplitude and phase response of the driving particle B1 as a function of the driving frequency in Fig. A(a) and (b), respectively. As expected, the amplitude decays with increasing frequency, while the phase is in sync with the drive at low frequencies and gradually lags behind as the frequency is increased.

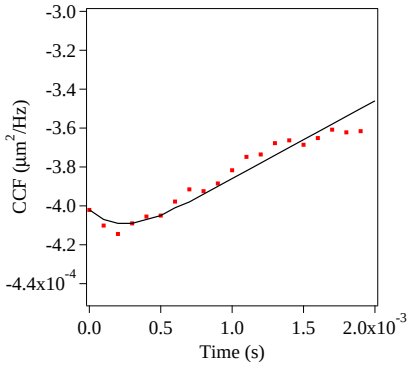

Figure 4. Position cross-correlation in time domain. The filled red squares are experimentally measured points, while the solid line is the theoretically calculated cross-correlation.

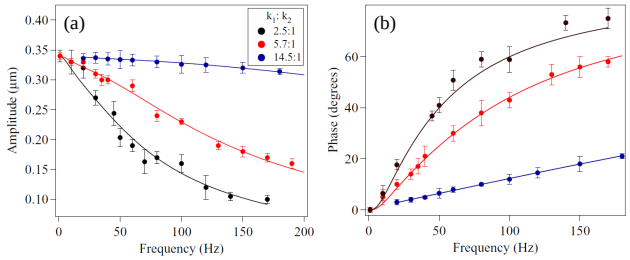

Figure 5. Amplitude (a) and phase (b) response of driving particle B1 as a function of drive frequency.

I. THEORY

We outline below key steps in deriving the response and correlations functions on the Smoluchowski time scale, *i.e.* the over-damped limit, starting from Langevin equations

$$m_i \dot{\boldsymbol{v}}_i + \boldsymbol{\gamma}_{ij} \cdot \boldsymbol{v}_j + \boldsymbol{\nabla}_i U = \boldsymbol{\xi}_i \tag{1}$$

presented and explained in the main text.

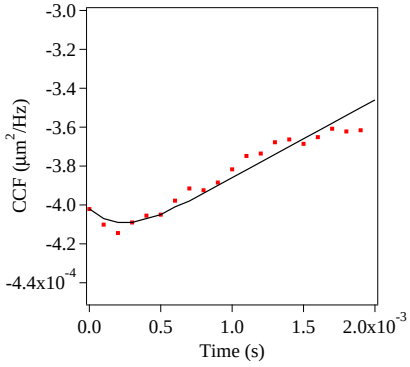

Figure 6. Position cross-correlation in time domain. The filled red squares are experimentally measured points, while the solid line is the theoretically calculated cross-correlation.

(*i*) *adiabatic elimination of momentum*: in the first step, the momenta $m_i\boldsymbol{v}_i$ are adiabatically eliminated from the Langevin equations to obtain a contracted description in terms of the positions alone [3, 4]. This equation is valid on time scales $t \gg m_i/\gamma_i$. The heuristic of setting $m_i\boldsymbol{v}_i$ to zero in the Langevin equations yields the same result as the more systematic adiabatic elimination procedure, provided the multiplicative noise is interpreted correctly and the so-called "spurious" drift is included in the equation for the position increment [5, 6]. With these caveats, the resulting over-damped Langevin equations are

$$\boldsymbol{\gamma}_{ij}\cdot\dot{\boldsymbol{r}}_j + \boldsymbol{\nabla}_i U = \boldsymbol{\xi}_i. \tag{2}$$

(*ii*) *linearization*: in the next step, the equations are linearized in the small displacements $\boldsymbol{r}_i(t) = \boldsymbol{r}_i^0 + \boldsymbol{u}_i(t)$, where $\boldsymbol{r}_i^0 + \boldsymbol{u}_i^0(t)$ is the *instantaneous* position of the trap center. The mean distance between the trap centers, $\boldsymbol{\rho} = \boldsymbol{r}_1^0 - \boldsymbol{r}_2^0$, is independent of time. This yields a linear equation of motion for the small displacements $\boldsymbol{u}_i$, where the friction tensors are now evaluated at the mean separation between the traps. The linearized Langevin equations are

$$\boldsymbol{\gamma}_{ij}(\boldsymbol{r}_1^0, \boldsymbol{r}_2^0)\cdot\dot{\boldsymbol{u}}_j + k_i\boldsymbol{u}_i - k_i\boldsymbol{u}_i^0(t) = \boldsymbol{\xi}_i \tag{3}$$

Note that these are 6 coupled stochastic ordinary differential equations.

(*iii*) *decoupling through the use of symmetries*: in this step, the symmetry of the friction tensors under translation, assuming all boundaries are remote, is used to express them as

$$\boldsymbol{\gamma}_{ij} = \gamma_{ij}^{\parallel}(\rho)\hat{\boldsymbol{\rho}}\hat{\boldsymbol{\rho}} + \gamma_{ij}^{\perp}(\rho)(\boldsymbol{I} - \hat{\boldsymbol{\rho}}\hat{\boldsymbol{\rho}}) \tag{4}$$

where $\gamma_{ij}^{||}(\rho)$ is the friction coefficient for relative motion along $\boldsymbol{\rho}$, the line joining the trap centers, while $\gamma_{ij}^{\perp}(\rho)$ is the corresponding quantity for motion perpendicular to $\boldsymbol{\rho}$. This motivates the decomposition of the displacement into components parallel and perpendicular to $\boldsymbol{\rho}$,

$$\boldsymbol{u}_i = u_i^{\parallel}\hat{\boldsymbol{\rho}} + \boldsymbol{u}_i^{\perp}\cdot(\boldsymbol{I} - \hat{\boldsymbol{\rho}}\hat{\boldsymbol{\rho}}). \tag{5}$$

Defining the force due to the driving of the trap as $\boldsymbol{f}_i(t) = k_i\boldsymbol{u}_i^0(t)$, averaging the equations over the noise, and using the two previous equations, we obtain 3 decoupled *pairs* of equations for each component of motion. For motion along the trap, the pair of coupled equations is

$$\gamma_{ij}^{||}\dot{u}_j^{||} + k_i u_i^{||} = f_i^{||}(t), \tag{6}$$

where the dependence of the friction coefficients on relative separation has been suppressed. The decoupling can be done before the linearization to give the same result; the two operations commute.

(iv) response function: in the final step the coupled equations are written as

$$\dot{u}_i^{||} + A_{ij}u_j^{||} = \mu_{ik}^{||}f_k \tag{7}$$

where $A_{ij} = \mu_{ij}^{||}k_j$ is a "response" matrix and the mobility matrix $\mu_{ij}^{||}$ is the inverse of the friction matrix, $\gamma_{ik}^{||}\mu_{kj}^{||}=\delta_{ij}$. The response function in the frequency domain, then, is [7]

$$\chi_{ij}^{||}(\omega) = (-i\omega\delta_{ik} + A_{ik})^{-1}\mu_{kj}^{||}. \tag{8}$$

Computing the inverse gives the following expression for the imaginary part of the response:

$$\mathrm{Im}\left[\chi_{ij}^{||}(\omega)\right] = \frac{\omega}{(\det A - \omega^2)^2 + (\omega\,\mathrm{tr}\,A)^2}\begin{pmatrix} \frac{k_2}{k_1}\mu_{22}^{\parallel}\det A + \mu_{11}^{\parallel}\omega^2 & -\mu_{12}^{\parallel}(\det A - \omega^2) \\ -\mu_{21}^{\parallel}(\det A - \omega^2) & \frac{k_1}{k_2}\mu_{11}^{\parallel}\det A + \mu_{22}\omega^2 \end{pmatrix}. \tag{9}$$

The modulus of the response of the first bead to the driving of the second bead is

$$|\chi_{21}^{||}| = \Big|\frac{i\omega\mu_{21}^{\parallel}}{\det A - \omega^2 - i\omega\,\mathrm{tr}\,A}\Big|, \tag{10}$$

which in non-zero only if there is viscous coupling, $\mu_{12}^{\parallel} \neq 0$. The modulus has a maximum at

$$\omega_{res} = \sqrt{\det A} = \sqrt{\mu_{11}^{\parallel}\mu_{22}^{\parallel}k_1k_2\left(1 - \frac{\mu_{12}^{\parallel}\mu_{21}^{\parallel}}{\mu_{11}^{\parallel}\mu_{22}^{\parallel}}\right)}. \tag{11}$$

(v) correlation function: To calculate the correlation function we set the modulation, $\boldsymbol{u}_i^0(t)$, of the traps to zero in Eq.(3) and project, as before, to obtain the Langevin equation for parallel displacement fluctuations

$$\boldsymbol{\gamma}_{ij}^{\parallel}\dot{u}_j^{\parallel}(t) + k_i u_i^{\parallel}(t) = \xi_i^{\parallel}(t), \tag{12}$$

$$\langle\xi_i^{\parallel}(t)\xi_j^{\parallel}(t')\rangle = 2k_BT\gamma_{ij}^{\parallel}\delta(t-t'). \tag{13}$$

The Fourier amplitudes of the displacements are

$$u_i^{\parallel}(\omega) = (-i\omega\delta_{il} + A_{il})^{-1}\mu_{lk}^{||}\xi_k^{\parallel}(\omega), \tag{14}$$

and the correlation function is then

$$C_{ij}(\omega) = \langle u_i^{\parallel}(\omega) u_j^{\dagger\parallel}(\omega)\rangle = (-i\omega\delta_{il} + A_{il})^{-1}\mu_{lk}^{||}\langle \xi_k \xi_{k'}\rangle \mu_{k'm}^{||}(+i\omega\delta_{mj} + A_{mj}^T)^{-1}. \tag{15}$$

Inserting the variance of the the noise, the correlation function is

$$C_{ij}(\omega) = \frac{2k_BT}{(\det A - \omega^2)^2 + (\omega \,\mathrm{tr}\, A)^2} \begin{pmatrix} \mu_{22}^{\parallel}k_2 - i\omega & -\mu_{12}^{\parallel}k_2 \\ -\mu_{21}^{\parallel}k_1 & \mu_{11}^{\parallel}k_1 - i\omega \end{pmatrix} \begin{pmatrix} \mu_{11}^{\parallel} & \mu_{12}^{\parallel} \\ \mu_{21}^{\parallel} & \mu_{22}^{\parallel} \end{pmatrix} \begin{pmatrix} \mu_{22}^{\parallel}k_2 + i\omega & -\mu_{21}^{\parallel}k_1 \\ -\mu_{12}^{\parallel}k_2 & \mu_{11}^{\parallel}k_1 + i\omega \end{pmatrix}. \tag{16}$$

Completing the matrix multiplications, the final result is

$$C_{ij}(\omega) = \frac{2k_BT}{\omega}\mathrm{Im}\left[\chi_{ij}^{||}(\omega)\right]. \tag{17}$$

This provides an explicit verification of the fluctuation-response relation for a pair of viscously coupled oscillators [8].

[1] A. B. Stilgoe, N. R. Heckenberg, T. A. Nieminen, and H. Rubinsztein-Dunlop, Phys. Rev. Lett. **107**, 248101 (2011).
[2] J.-C. Meiners and S. R. Quake, Physical Review Letters **82**, 2211 (1999).
[3] C. W. Gardiner, Phys. Rev. A **29**, 2814 (1984).
[4] C. W. Gardiner, *Handbook of stochastic methods*, Vol. 3 (Springer Berlin, 1985).
[5] N. G. van Kampen, J. Stat. Phys. **24**, 175 (1981).
[6] N. G. van Kampen, *Stochastic processes in physics and chemistry*, Vol. 1 (Elsevier, 1992).
[7] P. M. Chaikin and T. C. Lubensky, *Principles of condensed matter physics*, Vol. 1 (Cambridge Univ Press, 2000).
[8] R. Kubo, Rep. Prog. Phys. **29**, 255 (1966).